

## Ultrasonic attenuation due to H in a Pd<sub>85</sub>Pt<sub>15</sub> single crystal

This article has been downloaded from IOPscience. Please scroll down to see the full text article.

1992 J. Phys.: Condens. Matter 4 53

(<http://iopscience.iop.org/0953-8984/4/1/016>)

View [the table of contents for this issue](#), or go to the [journal homepage](#) for more

Download details:

IP Address: 171.66.16.159

The article was downloaded on 12/05/2010 at 10:59

Please note that [terms and conditions apply](#).

## Ultrasonic attenuation due to H in a Pd<sub>85</sub>Pt<sub>15</sub> single crystal

B Coluzzi, C Costa, A Biscarini and F M Mazzolai

Department of Physics, University of Perugia, via A Pascoli, 06100 Perugia, Italy

Received 18 April 1991, in final form 28 May 1991

**Abstract.** Ultrasonic attenuation has been measured as a function of temperature approximately over the range 10–300 K at 5, 10, 15 and 45 MHz in a single crystal of a Pd<sub>85</sub>Pt<sub>15</sub> alloy. The measurements have been carried out for five different propagation modes, both in the H-free and the H-loaded (H/(Pd + Pt) = 0.29 at. %) state of the material. An anelastic relaxation has been observed at around 225 K ( $f = 10$  MHz), whose activation energy  $W$  and limit relaxation time  $\tau_0$  are:  $W = 0.24 \pm 0.02$  eV;  $\tau_0 = (1.4 \pm 0.5) \times 10^{-14}$  s. The mode dependence of the relaxation strength reveals the existence of a hydrostatic relaxation due to reactions between dipoles associated with H–H and H–Pt complexes. The results can be accounted for in terms of stress-induced changes in the short-range order of both the H–H and the H–Pt bonds (or antibonds) as well as of the occupancy probabilities of octahedral interstitial sites by H.

### 1. Introduction

Anelastic relaxations due to stress-induced changes in the short-range order of H within the sublattice of the interstitial sites have been observed in a number of metal hydrides (Cannelli and Mazzolai 1964, Arons 1969, Mazzolai *et al* 1981, Mazzolai and Birnbaum 1985, Leisure *et al* 1983, Vajda *et al* 1983, Yoshinari and Koiwa 1986). The most extensively investigated hydride system is probably the  $\alpha'$ -phase of Pd, in which elastic after-effect, internal friction, and ultrasonic attenuation have been examined.

In the past few years some attention has been paid in our laboratory to the anelastic properties of Pd–M (M is a substitutional metal) alloys containing various amounts of H (Mazzolai and Lewis 1985, Mazzolai *et al* 1987, Sobha *et al* 1991). The relaxation processes observed in these ternary systems are rather complicated, due to the fact that both H–H and H–M complexes can give rise to stress-induced relaxation processes. In single crystals these relaxations can be distinguished from each other by propagating properly polarized ultrasonic pulses along principal crystal directions. Namely, H–H and H–M bonds (or antibonds) between nearest neighbours in a FCC lattice give rise to elastic dipoles of different symmetry (Nowick and Berry 1972).

In the present paper we report on ultrasonic propagation experiments carried out at MHz frequencies in a single crystal of Pd<sub>85</sub>Pt<sub>15</sub> alloy containing H. The main aims of this work were to investigate the symmetry properties of the relaxing defects and to characterize the H mobility over a wide temperature range. In order to accomplish the second goal, measurements of Gorsky relaxation and of internal friction in torsion at low frequencies have also been carried out and the results will be published shortly.

## 2. Experimental procedure

A Pd<sub>85</sub>Pt<sub>15</sub> single crystal supplied by Metals Research has been oriented and spark-erosion cut to have two parallel faces coinciding with (110) and (111) crystal planes. The specimen faces were parallel to within 10<sup>-5</sup> rad. After polishing, the specimen was annealed at 873 K for three hours at a pressure of 9 × 10<sup>-4</sup> Pa.

A H content  $n$  ( $n = H/(Pd + Pt)$ ) equal to an atomic ratio of 0.29 was introduced electrolytically. The density was measured by the hydrostatic balance method and was found to be 13.64 × 10<sup>3</sup> kg m<sup>-3</sup> in the annealed state and 12.94 × 10<sup>3</sup> kg m<sup>-3</sup> after H loading. The H and D contents were monitored through weight changes before and after electrolysation, as well as between consecutive measurement runs. These checks did not reveal any appreciable H or D losses.

The ultrasonic attenuation was recorded as a function of temperature in the range ≈ 10–293 K by means of an automatic attenuation recorder (Matec Model 2470 A). Five different propagation modes were used, whose appropriate relationships between the ultrasonic velocity,  $u$ , and the three elementary elastic constants  $C_{11}$ ,  $C_{12}$  and  $C_{44}$  are the following:

$$\begin{aligned} \rho u_{[110]}^2 &= \frac{1}{2}(C_{11} + C_{12} + 2C_{44}) = C_L \\ \rho u_{[111]}^2 &= \frac{1}{3}(C_{11} + 2C_{12} + 4C_{44}) = C^* \\ \rho u_{[110]}^{2[1\bar{1}0]} &= \frac{1}{2}(C_{11} - C_{12}) = C' & \rho u_{[110]}^{2[001]} &= C_{44} \\ \rho u_{[111]}^2 &= \frac{1}{3}(C_{11} - C_{12} + C_{44}) = C_T \end{aligned} \quad (1)$$

In the above relations the lower and upper indices indicate the propagation and the polarization directions, respectively. For the last mode the polarization direction was an arbitrary one in the (111) plane. An Au + 0.07 at. % Fe and chromel thermocouple was used to monitor the temperature.

## 3. Results

### 3.1. Attenuation data

In figures 1 to 5 the attenuation  $A$  (dB μs<sup>-1</sup>) divided by the angular frequency  $\omega$ , as measured at 10 or 15 MHz, both in the H-free and H-loaded specimen, is reported as a function of temperature for all the examined modes after background subtraction. A pronounced maximum is seen to occur at around 225 K.

To compare the present results with those of internal friction obtained in polycrystalline material, which will be discussed elsewhere, the coefficient of elastic energy dissipation,  $Q^{-1}$ , has been deduced from the attenuation coefficient  $A$  by using the following conversion formula:

$$Q^{-1} = A \text{ (dB } \mu\text{s}^{-1}\text{)}/4.35 \omega \text{ (Mrad s}^{-1}\text{)}. \quad (2)$$

It follows from this formula that the quantity  $A/\omega$  plotted as a function of  $T$  in figures 1 to 5 is proportional to  $Q^{-1}$ . The values  $Q_M^{-1}$  of  $Q^{-1}$  at the peak maximum are shown in table 1, where the measurement frequencies and the peak temperatures are also given. As can be seen,  $Q_M^{-1}$  is mode dependent and for mode  $C_L$ , for which measurements have been made at three different frequencies, it appears to be much smaller at 5 than at 15 and 45 MHz.

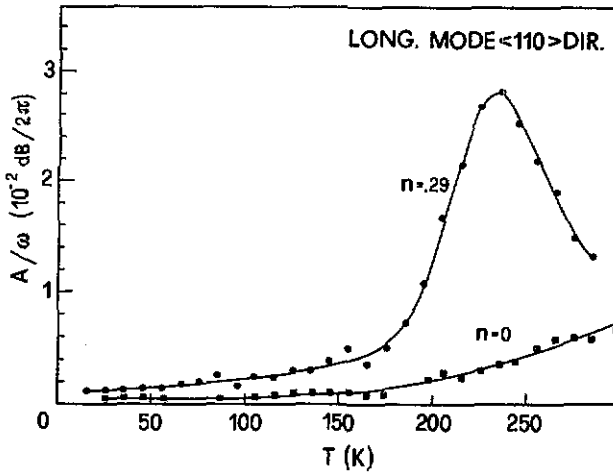


Figure 1. Temperature dependence of the attenuation coefficient  $A$  divided by the angular frequency  $\omega$  for the  $C_L$  propagation mode of the H-free and H-loaded specimen at a frequency of 15 MHz.

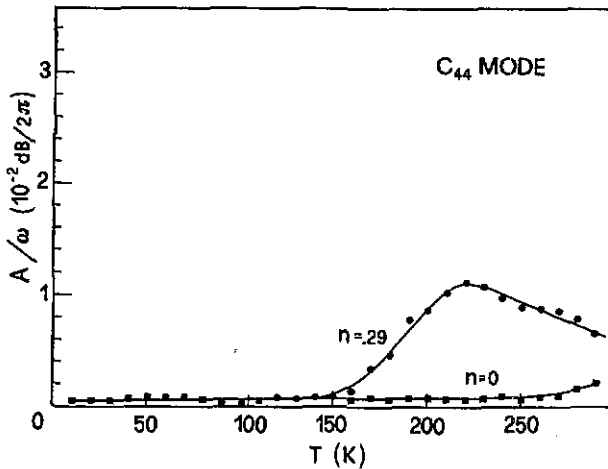


Figure 2. As in figure 1, but for the shear  $C_{44}$  mode.

### 3.2. Relaxation strength and spectrum of relaxation times

A composite Arrhenius plot is shown in figure 6, where some data obtained in the polycrystalline material at much lower frequencies are also included. The least squares fit of the data gives the following values for the activation energy  $W$  and the limit relaxation time  $\tau_0$ :

$$W = 0.24 \pm 0.02 \text{ eV} \quad \tau_0 = (1.4 \pm 0.5) \times 10^{-14} \text{ s.} \quad (3)$$

The limit relaxation time is of the order of magnitude expected for point defect relaxations, and the activation energy is only slightly lower than that for long-range diffusion in the  $\alpha'$  phase of Pd ( $W = 0.25 \text{ eV}$ ) (Völkl and Alefeld 1978).

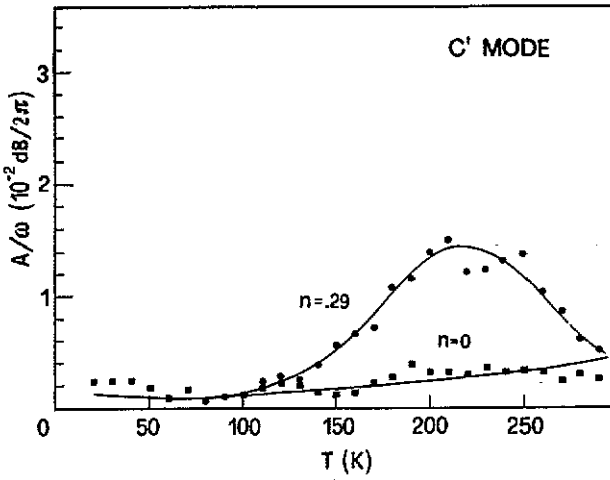


Figure 3. As in figure 1, but for the shear  $C'$  mode and a frequency of 10 MHz.

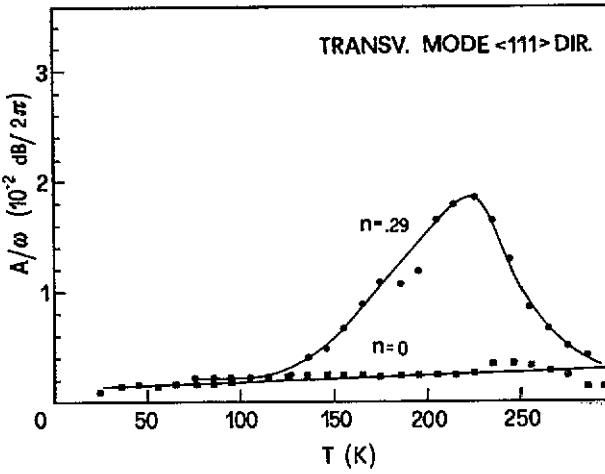


Figure 4. As in figure 1, but for the shear  $C_T$  mode and a frequency of 10 MHz.

Table 1. Temperature, frequency and height of the ultrasonic attenuation peak.

Mode	$T_M$ (K)	$f$ (MHz)	$Q_M^{-1} \times 10^5$
$C_L$	204	5	110
$C_L$	232	15	611
$C_L$	250	45	570
$C_M$	220	10	220
$C'$	225	10	275
$C_T$	225	15	379
$C^*$	225	15	106

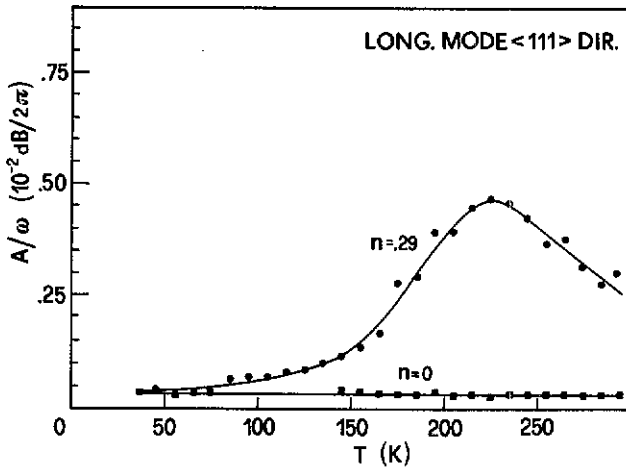


Figure 5. As in figure 1, but for the longitudinal C\* mode.

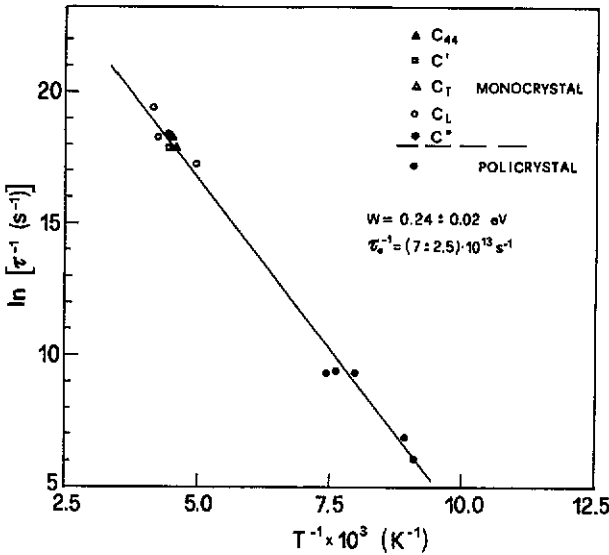


Figure 6. Arrhenius plot for the relaxation time, as determined by the ultrasonic pulse technique (at MHz frequencies) and by internal friction (at about 2000 and 60 Hz).

The width of the peaks shown in figures 1–5 is appreciably larger than expected for a single time relaxation process. By assuming a Gaussian distribution of the relaxation time spectrum we have calculated the half width,  $\beta$ , of the distribution and the associated value of the function  $f_2(0, \beta)$  (Nowick and Berry 1972, p 94), which characterizes the peak height, according to the relation:

$$Q_M^{-1} = S f_2(0, \beta). \tag{4}$$

The values of the relaxation strength  $S$  ( $S = \Delta C/C$ ) and of  $\beta$  are shown in table 2, where

**Table 2.** Relaxation strength and half width of the relaxation time spectrum.

Mode	$\beta$	$\beta^*$	$\Delta C/C \times 10^3$	$\Delta C/C \times 10^3^*$
$C_L$	1.7	1.20	17	2.8
$C_{44}$	2.1	1.63	7	3.1
$C'$	2.5	1.40	10	9.8
$C_T$	1.5	—	9	—
$C^*$	—	—	4	—
$B$	—	1.20	20	2.7

\* Data for a PdH<sub>0.67</sub> hydride (Leisure *et al* 1983).

data for a similar attenuation maximum observed in the  $\alpha'$  hydride of Pd are also given (Leisure *et al* 1983). It can be seen that, similar to  $Q_M^{-1}$ ,  $S$  is strongly mode dependent, the minimum and maximum values corresponding to  $C^*$  and  $C_L$  modes ( $f = 15$  MHz), respectively. Also the peak width is mode dependent and is larger for mode  $C'$  than  $C_{44}$ . It is worth noting that the relaxation strength for modes  $C_L$  and  $C_{44}$ , as well as the values of the spectrum width, are greater for this alloy than for Pd.

### 3.3. Self-consistency of the data and bulk modulus relaxation

According to relations (1) the relaxation strength  $\Delta C_T/C_T$  of mode  $C_T$  is given by:

$$\Delta C_T/C_T = (2\Delta C'/3C')(C'/C_T) + (\Delta C_{44}/3C_{44})(C_{44}/C_T). \quad (5)$$

The value of  $\Delta C_T/C_T$ , deduced from (5) using the relaxation strengths of table 2 and data on the elastic constants previously reported (Coluzzi *et al* 1989), is  $9 \times 10^{-3}$ , and compares favourably with that ( $10 \times 10^{-3}$ ) measured directly. This cross-check shows a consistency of the data for modes  $C_T$ ,  $C'$  and  $C_{44}$ .

From relations (1) the following expression can be deduced for  $C^*$ :

$$C^* = C_L - C' + C_T \quad (6)$$

which is found to be satisfied by our elastic constant data (Coluzzi *et al* 1989). However, the relaxation strength  $\Delta C^*/C^*$ , calculated from (6) is appreciably higher ( $16 \times 10^{-3}$ ) than that ( $4.3 \times 10^{-3}$ ) measured directly. There therefore seems to be an inconsistency between the data for  $C_L$  and  $C^*$  modes. Many series of measurements have been performed for mode  $C_L$  at 15 MHz, and they all give comparable results. It seems likely that the apparent discrepancy arises from uncertainties in the estimate of the height of the attenuation peak for mode  $C^*$ , which is relatively small with respect to the other peaks and to background subtracted, which for this mode was equal to  $3 \times 10^{-3}$ . Thus, in the following, the data for  $C^*$  mode will not be used for quantitative estimates.

From (1) the bulk modulus  $B$  ( $B = (C_{11} + 2C_{12})/3$ ) and its relaxation strength  $\Delta B/B$  can be expressed as follows:

$$B = C_L - (C'/3) - C_{44} \quad (7)$$

$$\Delta B/B = (\Delta C_L/C_L)(C_L/B) - (\Delta C_{44}/C_{44})(C_{44}/B) - (\Delta C'/C')(C'/3B). \quad (8)$$

The value of  $\Delta B/B$  deduced from (8) ( $20 \times 10^{-3}$ ) is markedly higher than that found for the Pd hydride (Leisure *et al* 1983).

**Table 3.** (a) Fractions of interstitial sites ( $p_i$ ) and of H atoms ( $c_i/n$ ) over sites  $I_i$  at 225 K. (b) Transition probability factor  $c_i q_{ij}(1 - c_j/p_j)/n$  at 225 K.

(a)					
$i$	6	5	4 ort.	4 tetr.	3
$p_i$	0.377	0.399	0.141	0.035	0.041
$c_i/n$	0.963	0.037	<0.001	<0.001	<0.001
(b)					
$i/j$	6	5	4 ort.	4 tetr.	3
6	0.131	0.345	0.078	0.016	0.011
5	0.003	0.015	0.005	0.002	0.001
4 ort.	<0.001	<0.001	<0.001	<0.001	<0.001
4 tetr.	<0.001	<0.001	<0.001	<0.001	<0.001

## 4. Discussion

### 4.1. General features of the PdPtH system

Information available in the literature shows that the addition of platinum to palladium appreciably reduces the critical temperature  $T_c$  and the critical concentration  $n_c$  of H in the PdPtH system. For the alloy used in this work rough estimates of  $T_c$  and  $n_c$ , based on  $p$ - $T$ - $n$  curves of Carson *et al* (1960), are 225 K and 0.08, respectively. Thus, for the H content of the present experiment ( $n = 0.29$ ), the system is expected to be a homogeneous  $\alpha'$  phase in the temperature range of the relaxation process. The dependence on Pt content of the enthalpies of solution and diffusion of H has been investigated by McLellan and co-workers (Yoshihara and McLellan 1986, McLellan and Yoshihara 1987). A marked increase of both the solution and diffusion enthalpies on Pt content is found, particularly for values of the atomic concentration higher than 0.10.

### 4.2. Interstitial sites

It has become apparent from some relatively recent works (Kirchheim 1982, Brouwer *et al* 1988, Sobha *et al* 1991) that the solubility and diffusion features of H in alloys is intimately related to the nature of the interstitial sites available for H. In a FCC alloy, seven different interstitial sites  $I_i$  can be distinguished on the basis of the number  $i$  ( $i = 0, 1 \dots 6$ ) of Pd atoms occupying the nearest-neighbour lattice sites of an interstice. The number of distinguishable sites becomes ten if the symmetry features associated with the distribution of Pt atoms among the six nearest lattice sites are also taken into account (Hohler and Kronmüller 1982). The  $I_6$  site has cubic symmetry, the  $I_5$  tetragonal, while the  $I_4$  can be either tetragonal or orthorhombic. In its tetragonal and orthorhombic configurations the  $I_4$  site has the two Pt atoms respectively aligned along [100] and [110] crystal directions. In a random alloy the fractions  $p_i$  of sites  $I_i$  for  $i \geq 3$  are given in table 3(a).

Neglecting second and more distant neighbours, the local concentration  $x_i$  of Pt around a site  $I_i$  is  $(6 - i)/6$ . The fractions  $c_i$  of the occupied sites have been deduced (Coluzzi *et al* 1992) (see table 3(a)) using Fermi-Dirac statistics and the site energies calculated from the embedded cluster model introduced by Griessen (1986). The fraction



$c_i$  is the number of interstitial atoms  $n_i$  on sites of type  $i$  divided by the total number of interstitial sites  $M$ . The probability of stress-assisted transitions from one site of type  $i$  to a nearest-neighbour site of type  $j$  is proportional to  $c_i$  and to the probability  $q_{ij}(1 - c_j/p_j)$  of finding an empty site of type  $j$  as nearest neighbour of a site of type  $i$ ;  $c_j/p_j$  is the fractional occupation of sites  $j$  and  $(1 - c_j/p_j)$  the probability that site  $j$  is empty. Thus, following a procedure already applied to BCC alloys (Brouwer *et al* 1988), the quantities  $q_{ij}$  have been calculated as a function of the overall Pt content  $x$  (Coluzzi *et al* 1992). For the composition of the present alloy Pd<sub>85</sub>Pt<sub>15</sub>, the transition probability factors  $c_i q_{ij}(1 - c_j/p_j)/n$  are listed in table 3(b). It may be seen from this table that for  $i < 5$  and  $j < 4$  the probabilities for transitions from sites  $I_i$  towards sites  $I_j$  are small and will be neglected in the following discussion.

### 4.3. Main features and possible mechanisms of the relaxation

**4.3.1. Role of Pt-H bonds (or antibonds).** The relaxation strengths for  $C_{44}$  and  $C'$  modes in the presence of reacting isotropic and tetragonal dipoles have been calculated and are reported in the appendix. The results of such calculations, when adapted to include the blocking effects and the geometrical restrictions involved in the nature of  $I_6$ ,  $I_5$  and  $I_4$  dipoles, become:

$$\frac{\Delta C_{44}}{C_{44}} = -C_{44} \frac{v_0}{3kTc_t} \frac{1}{2} \sum_{l,r=4}^6 \pi_{lr} \pi_{rl} (\text{tr } \lambda^{(l)} - \text{tr } \lambda^{(r)})^2 \quad (9)$$

$$\Delta C'/C' = (\Delta C_{44}/C_{44})(C'/C_{44}) - C'(2v_0/3kT) \times [\pi'_{44}(\lambda_1^{(4)} - \lambda_2^{(4)})^2 + \pi'_{55}(\lambda_1^{(5)} - \lambda_2^{(5)})^2] \quad (10)$$

where  $\pi_{lr} = c_l q_{lr}(1 - c_r/p_r)$  is the fraction of the  $I_l$  dipoles that can react with the  $I_r$ ,  $c_t = \sum_{l,r=4}^6 \pi_{lr}$  the cumulative fraction of all the reacting dipoles,  $\text{tr } \lambda^{(l)} = \lambda_1^{(l)} + \lambda_2^{(l)} + \lambda_3^{(l)}$  the trace of the  $\lambda$  tensor associated with dipole  $I_l$  (Nowick and Heller 1963) and  $\lambda_j^{(l)}$  its principal values,  $v_0$  the atomic volume of the alloy,  $k$  the Boltzmann constant, and  $T$  the absolute temperature. The fractions of the  $I_4$ - $I_4$  and  $I_5$ - $I_5$  transitions leading to reorientation only differ slightly from  $\pi_{44}$  and  $\pi_{55}$  and have been denoted as  $\pi'_{44}$  and  $\pi'_{55}$  in relation (10).

From a comparison of (9) with results by Nowick and Heller (1963) concerning bulk modulus relaxation under a hydrostatic stress, it turns out that:

$$\Delta C_{44}/C_{44} = (\Delta B/B)(C_{44}/3B). \quad (11)$$

It is to be noted that, unlike in the case of isolated defects, reacting dilation centres ( $\lambda_1^{(l)} = \lambda_2^{(l)} = \lambda_3^{(l)} = \lambda^{(l)}$ ) and tetragonal dipoles ( $\lambda_1^{(l)} \neq \lambda_2^{(l)} = \lambda_3^{(l)} = \lambda^{(l)}$ ) can also give rise to relaxation for mode  $C_{44}$  provided a difference exists between the traces of their  $\lambda$  tensors. It is worth noting that, while the relaxation of  $C'$  is due to either the reorientation or reaction processes, the relaxations of  $C_{44}$  and  $B$  only probe reactions. According to (10) a larger relaxation strength and a wider spectrum of relaxation times are expected for the  $C'$  than the  $C_{44}$  mode. This is in agreement with experiment, as shown in table 2. Including the orthorhombic dipole  $I_4$  in the model would result in additional terms: three for the reactions and one for the reorientation. This last term contributes to the relaxation of  $C_{44}$  but not to that of  $B$  (Nowick and Heller 1963), making relations (10) and (11) invalid. Actually, the value obtained for  $\Delta B/B$  ( $60 \times 10^{-3}$ ) by inserting the directly measured value of  $\Delta C_{44}/C_{44}$  into relation (11) is three times higher

than that estimated in the previous section ( $20 \times 10^{-3}$ ). This is probably due to a contribution to  $\Delta C_{44}/C_{44}$  from the reorientation of orthorhombic dipoles such as  $I_4$ . However, the difference is so large that it seems likely that other orthorhombic defects associated with H also contribute to the relaxation in this alloy. It can thus be concluded that the experimental results cannot be fully explained solely in terms of the changes in the short-range order of H–Pt bonds (or antibonds).

**4.3.2. Role of H–H bonds.** Similarly to what has been done in the case of the Pd hydride, an additional mechanism is to be considered for the relaxation; that is, the changes, induced by the applied stress, of the directional short-range order along the  $\langle 110 \rangle$  directions of the H–H bonds formed by nearest-neighbour interstitial atoms. This mechanism is expected (LeClaire and Lomer 1954, Welch and LeClaire 1967) to give rise to a relaxation of  $C'$ ,  $C_{44}$  and of the bulk modulus  $B$ . Thus, in principle, it appears to be suitable for qualitatively interpreting the main observations made in the course of the present investigation. However, there are indications that this cannot be the only mechanism operating. For example, the values of the ratios  $(\Delta C_{44}/C_{44})/(\Delta B/B)$  and  $(\Delta C'/C')/(\Delta B/B)$  as deduced from table 2 are much smaller in the case of the Pd<sub>85</sub>Pt<sub>15</sub> alloy than in the case of pure Pd. This strongly suggests that in the alloy a large contribution to the bulk modulus relaxation arises from stress-induced dipole-dipole reactions involving H–Pt complexes, as discussed above. This view is further supported by the fact that the parameter  $\beta$ , which gives a measure of the width of the Gaussian distribution of the relaxation times, also takes larger values in the case of Pd<sub>85</sub>Pt<sub>15</sub> than in the  $\alpha'$  hydride of pure Pd, as seen in table 2.

**4.3.3. Relaxation kinetics.** As noted in previous sections the activation energy for H diffusion in the present alloy is close to that measured in the  $\alpha$  ( $W = 0.23$  eV) and  $\alpha'$  ( $W = 0.25$  eV) phases of Pd. At first sight this may seem surprising in view of the strong interaction of Pt atoms with H, as demonstrated by the marked dependence on Pt content of the H solubility in PdPt alloys (Carson *et al* 1960). A possible explanation of this close coincidence is the fact that H is mostly distributed among  $I_6$ ,  $I_5$  and  $I_4$  sites and the jumps from one site to the other occur in a richer palladium environment than that indicated by the nominal composition of the alloy. This result is further indirect proof that  $I_6$ ,  $I_5$  and  $I_4$  dipoles play the dominant role in the observed anelasticity.

As shown in table 1 the peak temperature is slightly lower for the  $C_{44}$  than the  $C'$  mode. This observation can be easily accounted for in terms of H–Pt complexes. Namely, the reorientation of the tetragonal  $I_4$  dipoles, which does not affect  $C_{44}$  relaxation, is expected to be of higher energy (Coluzzi *et al* 1992), thus contributing to the high temperature side of the peak.

## 5. Conclusions

The main results of the present investigation can be summarized as follows:

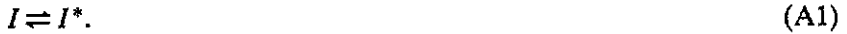
(i) A large relaxation exists within the  $\alpha'$  phase of PdPt alloys for all the examined modes, including the hydrostatic one.

(ii) Calculations show that the reaction of a dilation centre with a tetragonal dipole, can give rise to the relaxation of both the shear elastic constant  $C_{44}$  and the bulk modulus  $B$ , and also contributes to the relaxation of  $C'$ .

(iii) The conclusion can be drawn that an applied stress induces changes in the degree of directional short-range order of both the Pt-H and H-H bonds (or antibonds), respectively along  $\langle 100 \rangle$  and  $\langle 110 \rangle$  directions.

### Appendix: Relaxation of the elastic compliances $s_{ijkl}$ due to cubic and tetragonal reacting dipoles under a uniaxial stress in cubic crystals

Let us consider two dipole species  $I$  and  $I^*$  with  $n'$  and  $n^*$  number of crystallographically equivalent orientations, that under an applied stress can be transformed one into the other according to the reaction:



The relaxation,  $\delta s_{ijkl}$ , of the compliance component  $s_{ijkl}$  is given by (Nowick and Heller 1963):

$$\begin{aligned} \delta s_{ijkl} = & \frac{v_0 c_0}{kT n'} \left[ \sum_p \lambda_{ij}^{(p)} \lambda_{kl}^{(p)} - \frac{c_0}{n' c_t} \left( \sum_p \lambda_{ij}^{(p)} \right) \left( \sum_q \lambda_{kl}^{(q)} \right) \right] \\ & + \frac{v_0 c_0^*}{kT n^*} \left[ \sum_r \lambda_{ij}^{*(r)} \lambda_{kl}^{*(r)} - \frac{c_0^*}{n^* c_t} \left( \sum_r \lambda_{ij}^{*(r)} \right) \left( \sum_s \lambda_{kl}^{*(s)} \right) \right] \\ & - \frac{v_0 c_0 c_0^*}{kT n' n^* c_t} \left[ \left( \sum_p \lambda_{ij}^{(p)} \right) \left( \sum_r \lambda_{kl}^{*(r)} \right) + \left( \sum_p \lambda_{kl}^{(p)} \right) \left( \sum_r \lambda_{ij}^{*(r)} \right) \right] \end{aligned} \quad (\text{A2})$$

where  $v_0$  is the atomic (or molecular) volume;  $\lambda_{ij}^{(p)}$  ( $\lambda_{ij}^{*(p)}$ ) the component of the elastic dipole tensor  $\lambda$  ( $\lambda^*$ ) for the dipole orientation  $p$ ;  $c_0$  and  $c_0^*$  the molar concentrations of the two species  $I$  and  $I^*$ , whose sum, taking the total number of dipoles as constant, has been denoted as:

$$c_t = c_0 + c_0^*. \quad (\text{A3})$$

The relation (A2), specialized to the case of a homogeneous uniaxial stress  $\sigma$ , becomes:

$$\begin{aligned} \delta J = & \frac{v_0 c_0}{kT n'} \left[ \sum_p (\lambda^{(p)})^2 - \frac{c_0}{n' c_t} \left( \sum_p \lambda^{(p)} \right)^2 \right] \\ & + \frac{v_0 c_0^*}{kT n^*} \left[ \sum_r (\lambda^{*(r)})^2 - \frac{c_0^*}{n^* c_t} \left( \sum_r \lambda^{*(r)} \right)^2 \right] \\ & - 2 \frac{v_0 c_0 c_0^*}{kT n' n^* c_t} \left[ \left( \sum_p \lambda^{(p)} \right) \left( \sum_r \lambda^{*(r)} \right) \right] \end{aligned} \quad (\text{A4})$$

where  $\lambda^{(p)}$  ( $\lambda^{*(p)}$ ) denotes the component of  $\lambda$  ( $\lambda^*$ ) corresponding to  $\sigma$ , and  $\delta J$  the relaxation of the compliance  $J$ . The component  $\lambda^{(p)}$  can be expressed in terms of the principal values  $\lambda_i$  ( $i = 1, 2, 3$ ) of  $\lambda$  according to the relation:

$$\lambda^{(p)} = (\alpha_1^{(p)})^2 \lambda_1 + (\alpha_2^{(p)})^2 \lambda_2 + (\alpha_3^{(p)})^2 \lambda_3 \quad (\text{A5})$$

where the  $\alpha_i^{(p)}$  ( $i = 1, 2, 3$ ) are the direction cosines between the stress axis and the three principal axes of the  $\lambda$  tensor for the dipole orientation  $p$ . A similar relation holds for

$\lambda^{*(p)}$ . If  $\sigma$  is applied to a cubic crystal along  $\langle 100 \rangle$  or  $\langle 111 \rangle$  directions and  $I$  and  $I^*$  are respectively tetragonal ( $\lambda_1 \neq \lambda_2 = \lambda_3$ ) and cubic ( $\lambda_1^* = \lambda_2^* = \lambda_3^* = \lambda^*$ ) dipoles, then

$$\delta J_{\langle 100 \rangle} = \delta s' / 3 = -(1/3C')(\Delta C' / C') \quad (A6)$$

$$\delta J_{\langle 111 \rangle} = \delta s / 3 = -(1/3C_{44})(\Delta C_{44} / C_{44}). \quad (A7)$$

A tetragonal dipole has its principal axes aligned along the cube axes, thus, the direction cosines for  $[111]$  and  $[100]$  uniaxial stresses are:

$$\alpha_i^{(p)} = 1/\sqrt{3} \quad i, p = 1, 2, 3 \quad (A8)$$

and

$$\alpha_i^{(1)} = \delta_{i1} \quad \alpha_i^{(2)} = \delta_{i2} \quad \alpha_i^{(3)} = \delta_{i3} \quad (A9)$$

respectively. Here  $\delta_{ij}$  is the Kronecker symbol. For the dilation centre  $I^*$ ,  $n^*$  is equal to 1. Using relations from A5 to A9 we get:

$$\delta s' = \frac{1}{3}(v_0/kT)(c_0 c_0^* / c_t)[\delta \text{tr } \lambda]^2 + \frac{2}{3}(v_0/kT)c_0(\lambda_1 - \lambda_2)^2 \quad (A10)$$

$$\delta s = \frac{1}{3}(v_0/kT)(c_0 c_0^* / c_t)[\delta \text{tr } \lambda]^2. \quad (A11)$$

If the two species  $I$  and  $I^*$  in the reaction (A1) were two different tetragonal dipole species, following the preceding procedure, an expression identical to (A11) is found for  $\delta s$ , while  $\delta s'$  turns out to be given by:

$$\delta s' = \delta s + \frac{2}{3}(v_0/kT)c_0(\lambda_1 - \lambda_2)^2 + \frac{2}{3}(v_0/kT)c_0^*(\lambda_1^* - \lambda_2^*)^2. \quad (A12)$$

Each tetragonal species appears to contribute to  $\delta s'$  with its reorientation term.

Finally, consider the case of  $l$  different tetragonal dipole species  $I_r$  and  $m$  cubic dipole species  $I_r^*$  that can simultaneously transform one into the other by a reaction of type (A1). Neglecting interactions, each of the possible reactions can be treated separately (Nowick and Heller 1963) to give:

$$\delta s = \frac{v_0}{3kTc_t} \frac{1}{2} \sum_{r,s=1}^{l+m} c_r c_s [\text{tr } \lambda^{(r)} - \text{tr } \lambda^{(s)}]^2 \quad (A13)$$

$$\delta s' = \delta s + \frac{2}{3} \frac{v_0}{kT} \sum_{r=1}^l c_r (\lambda_1^{(r)} - \lambda_2^{(r)})^2 \quad (A14)$$

where  $c_t$  is given now by:

$$c_t = \sum_{r=1}^{l+m} c_r. \quad (A15)$$

### Acknowledgments

We are grateful to Professor L Passari of University of Ferrara for having given us the single crystal and to Professor H K Birnbaum of University of Illinois for having allowed us to use the facilities for sample preparation available at MRL. We also acknowledge technical assistance by S Agabiti, E Babucci, G Chiocci and G Piluso.

## References

- Arons R R 1969 *PhD Thesis* Amsterdam University
- Brouwer R C, Salomons E and Griessen R 1988 *Phys. Rev.* **38** 10217–26
- Cannelli G and Mazzolai F M 1964 *Nuovo Cimento* **64B** 171–80
- Carson A W, Flanagan T B and Lewis F A 1960 *Trans. Faraday Soc.* **56** 1332–39
- Coluzzi B, Costa C, Marzola P and Mazzolai F M 1989 *J. Phys.: Condens. Matter* **1** 6335–42
- Griessen R 1986 *Hydrogen in Disordered and Amorphous Solids* ed G Bambakidis and R C Bowman (New York: Plenum) pp 153–72
- Hohler B and Kronmüller H 1982 *Phil. Mag.* **45** 607–23
- Kirchheim R 1982 *Acta Metall.* **30** 1069–78
- LeClaire A D and Lomer W M 1954 *Acta Metall.* **2** 731–42
- Leisure R G, Kanashiro T, Riedi P C and Hsu D K 1983 *Phys. Rev.* **B 27** 4872–82
- Mazzolai F M and Birnbaum H K 1985 *J. Phys. F: Met. Phys.* **15** 525–42
- 1985 *J. Phys. F: Met. Phys.* **15** 507–23
- Mazzolai F M, Bordoni P G and Lewis F A 1981 *J. Phys. F: Met. Phys.* **11** 337–52
- Mazzolai F M and Lewis F A 1985 *J. Phys. F: Met. Phys.* **15** 1261–77
- Mazzolai F M, Lewis F A and Marzola P 1987 *J. Physique Coll.* **48** C8 269–74
- McLellan R B 1982 *Acta Metall.* **30** 317–22
- McLellan R B and Yoshihara M 1987 *Acta Metall.* **35** 197–225
- Nowick A S and Berry B S 1972 *Anelastic Relaxation in Crystalline Solids* (New York: Academic)
- Nowick A S and Heller W R 1963 *Adv. Phys.* **12** 251–98
- Sobha B, Coluzzi B, Mazzolai F M, Flanagan T B and Sakamoto Y 1991 *J. Less-Common Met.* **172** 254
- Vajda P, Daou J N and Moser P 1983 *J. Phys.* **44** 543
- Vökl J and Alefeld G 1978 *Hydrogen in Metals I*, vol 28 *Topics in Applied Physics* ed Alefeld G and Vökl J (New York: Springer) p 321
- Welch D O and LeClaire A D 1967 *Phil. Mag.* **16** 981–1008
- Yoshihara M and McLellan R B 1986 *Acta Metall.* **34** 1359–66
- Yoshinari O and Koiwa M 1986 *Acta Metall.* **30** 1979–86